

SCIENTIFIC REPORTS

OPEN

Seed priming with polyethylene glycol regulating the physiological and molecular mechanism in rice (*Oryza sativa* L.) under nano-ZnO stress

Sheteiwy Mohamed Salah^{1,2}, Guan Yajing¹, Cao Dongdong³, Li Jie¹, Nawaz Aamir^{1,4}, Hu Qijuan¹, Hu Weimin¹, Ning Mingyu⁵ & Hu Jin¹

Received: 12 May 2015

Accepted: 21 August 2015

Published: 30 September 2015

The present study was designed to highlight the impact of seed priming with polyethylene glycol on physiological and molecular mechanism of two cultivars of *Oryza sativa* L. under different levels of zinc oxide nanorods (0, 250, 500 and 750 mg L⁻¹). Plant growth parameters were significantly increased in seed priming with 30% PEG under nano-ZnO stress in both cultivars. Whereas, this increase was more prominent in cultivar Qian You No. 1 as compared to cultivar Zhu Liang You o6. Significant increase in photosynthetic pigment with PEG priming under stress. Antioxidant enzymes activities of superoxide dismutase (SOD), peroxidase (POD) and catalase (CAT) as well as malondialdehyde (MDA) contents were significantly reduced with PEG priming under nano-ZnO stress. Gene expression analysis also suggested that expression of *APXa*, *APXb*, *CATa*, *CATb*, *CATc*, *SOD1*, *SOD2* and *SOD3* genes were down regulated with PEG priming as compared to non-primed seeds under stress. The ultrastructural analysis showed that leaf mesophyll and root cells were significantly damaged under nano-ZnO stress in both cultivars but the damage was prominent in Zhu Liang You o6. However, seed priming with PEG significantly alleviate the toxic effects of nano-ZnO stress and improved the cell structures of leaf and roots in both cultivars.

Plants exposed to high concentrations of heavy metals experience changes in physiological, biochemical and molecular mechanisms of plant cells¹. Uptake of nanoparticles (NPs) through primary roots is usually barred due to presence of suberized exo- and endodermis. However, lateral root junctions are the primary sites through which NPs could enter the xylem via cortex and the central cylinder². The higher concentrations of titanium dioxide (TiO₂) enhanced the alterations in mitotic activity and chromosomal aberrations, indicating genotoxic effects of nanoparticles (NPs)³. Nano-ZnO stress shows more detrimental effects on germination and root growth of rice as compared to TiO₂ nanoparticles⁴. Recently, Ng *et al.* studied the molecular downstream effects of ZnO nanoparticles on p53 signaling pathways, suggesting that ZnO nanoparticles might be sufficiently genotoxic to stimulate the DNA damage machinery and it might have caused DNA lesions because p53 was upregulated and phosphorylated with a concomitant decrease in cell cycle progression after seven days⁵. Furthermore, Giovanni *et al.* found that noncytotoxic zinc oxide NPs level (10 mg/L) could elevate the intracellular oxidative stress⁶. It has been observed that

¹Seed Science Center, College of Agriculture and Biotechnology, Zhejiang University, Hangzhou 310058, China.

²Department of Agronomy, Faculty of Agriculture, Mansoura University, Mansoura 35516, Egypt. ³Zhejiang Nongke Seed Industry Limited Company, Hangzhou, 310021, China. ⁴Faculty of Agricultural Sciences and Technology, Bahauddin Zakariya University Multan, 60000 Pakistan. ⁵National Agricultural Technology Extension Service Center, China. Correspondence and requests for materials should be addressed to H.J. (email: jhu@zju.edu.cn)

Cultivars	Priming with PEG (%)	nano-ZnO conc. (mg L ⁻¹)	GP (%)	GI	EG (%)	MGT (days)	Leaf surface area (cm ²)
Zhu Liang You 06	0	0	90.00 ± 2.00 e	96.66 ± 2.30 a-c	81.33 ± 2.30 g	6.13 ± 0.05 f	3.30 ± 0.11 i
		250	86.00 ± 3.46 f	95.00 ± 2.00 bc	76.00 ± 4.00 h	7.19 ± 0.08 c	2.65 ± 0.39 j
		500	82.00 ± 3.46 g	90.33 ± 4.50 d	76.00 ± 0.05 h	7.71 ± 0.10 b	2.67 ± 0.04 j
		750	52.00 ± 2.00 j	57.33 ± 3.21 g	72.00 ± 0.09 i	8.53 ± 0.32 a	2.45 ± 0.13 j
	30	0	95.33 ± 1.15 b-d	98.33 ± 0.57 ab	100.00 ± 0.04 a	4.53 ± 0.25 j	4.95 ± 0.05 d
		250	93.33 ± 1.15 c-e	97.00 ± 0.08 a-c	94.66 ± 2.30 cd	5.50 ± 0.10 h	4.60 ± 0.10 e
		500	92.00 ± 0.05 de	94.33 ± 2.30 bc	92.00 ± 0.08 de	6.30 ± 0.10 ef	4.23 ± 0.20 fg
		750	66.00 ± 2.00 h	68.66 ± 3.05 f	88.00 ± 0.07 f	6.88 ± 0.07 d	4.03 ± 0.05 gh
Qian You No. 1	0	0	96.00 ± 0.05 bc	96.00 ± 0.03 a-c	96.00 ± 4.00 bc	5.43 ± 0.14 h	4.41 ± 0.10 ef
		250	92.00 ± 0.03 de	95.00 ± 0.08 bc	96.00 ± 0.08 bc	5.80 ± 0.10 g	4.13 ± 0.15 gh
		500	90.00 ± 0.05 e	93.00 ± 0.07 cd	90.66 ± 2.30 ef	6.38 ± 0.07 e	3.88 ± 0.07 h
		750	58.00 ± 2.08 i	60.00 ± 2.00 g	88.00 ± 0.07 f	6.88 ± 0.07 d	3.38 ± 0.02 i
	30	0	100.00 ± 0.06 g	100.00 ± 0.07 a	100.00 ± 0.09 a	4.16 ± 0.03 k	5.90 ± 0.10 a
		250	98.00 ± 0.05 ab	98.00 ± 0.09 ab	100.00 ± 0.09 a	4.71 ± 0.10 j	5.61 ± 0.17 b
		500	98.00 ± 0.07 ab	98.00 ± 0.07 ab	99.00 ± 0.05 ab	5.14 ± 0.05 i	5.26 ± 0.05 c
		750	84.00 ± 4.00 fg	84.00 ± 4.00 e	98.00 ± 0.07 ab	5.40 ± 0.10 h	5.03 ± 0.05 cd

Table 1. Effect of seed priming with PEG (30%) on germination percentage (GP%), germination index (GI), Energy of germination (EG%), mean germination time (MGT d.) and leaf surface area (cm²) of two rice cultivars under different ZnO nanorods concentrations. The same letters within a column indicate there was no significant difference at a 95% probability level at the $p < 0.05$ level, respectively.

higher concentrations (2000 mg/L) of nano-Zn (35 nm) and ZnO (20 nm) inhibit the germination in ryegrass and corn, respectively⁷. Moreover, root length of the studied species was also inhibited with use of 200 mg/L nano-Zn and ZnO. In addition, phytotoxicity of nano-Al and Al₂O₃ significantly affect the root elongation of ryegrass and corn, and nano-Al enhance the root growth of radish and rape⁸. The physiology and biochemistry of the toxic effects of Zn in plants were likely to be similar to those reported for other heavy metals. In this regard, Chia *et al.* reported that ZnO NMs exert their toxic effects intracellularly⁹. However, Zn is not considered to be highly phytotoxic¹⁰.

Seed priming could be defined as a technique that controls the hydration level within seeds induce metabolic activities for germination but radical emergence is prevented. Previous studies have revealed that rice seed priming can enhance seed germination, vigour index and germination energy¹¹. Polyethylene glycol (PEG) has been used frequently in plant water deficit studies to induce dehydration by decreasing water potential¹². It is observed that priming with PEG can shorten the time to seed emergence and increases the germination percentage¹³, and improves salt tolerance¹⁴. Moreover, seed priming with PEG enhances the chilling tolerance¹⁵.

Zinc uptake in plants is critical as it plays many essential unique biological functions. The vast array of proteins use zinc for stabilizing their structures because it possesses in a functional form¹⁶. Zinc has major contribution to perform biochemical and physiological processes, even slight deficiencies may affect growth and yield. These all evidences inspired us to understand the molecular mechanisms of nano-ZnO uptake, translocation and storing of zinc in rice plants. This study provides new information on nanotoxicology, as we investigated the effects of seed priming with PEG on seed vigor, antioxidant enzyme activities and their gene expression of two rice cultivars under nano-ZnO stress. Moreover, the induction of antioxidative defense was also investigated at enzymatic as well as transcriptional level in order to disclose the toxicity mechanisms of ZnO in rice plants. This approach may enhance our understandings about the toxicity of engineered nanoparticles (ENPs) on this plant species. Thereafter, it could be helpful to improve the plant growth in ZnO polluted soils.

Results

Seed vigour and plant growth. The present study showed that germination percentage, germination index and energy of germination were significantly reduced at higher level of ZnO (750 mg L⁻¹) in both cultivars over their respective controls (Table 1). The results also revealed that there was a significant difference in mean values of germination percentage, germination index and energy of germination which showed decreasing trend with an increase in ZnO concentrations and this decline was more obvious in cultivar Zhu Liang You 06 as compared with cultivar Qian You No. 1. As far as PEG priming was concerned, the result showed that seed priming with PEG (30%) resulted in a significant resistance to nano-ZnO stress (Table 1). Seed priming has been shown promising for hastening seed germination under stress as compared to the control in both cultivars. Likewise, leaf surface area was also statistically

Cultivars	Priming with PEG (%)	nano-ZnO conc. (mg L ⁻¹)	Root length (cm)	Shoot length (cm)	SFW (g)	SDW (g)	SVI
Zhu Liang You 06	0	0	9.16 ± 0.61 f-h	7.33 ± 0.15 de	0.073 ± 0.01 fg	0.043 ± 0.02 b	1484 ± 29.6 f
		250	8.60 ± 0.36 h-j	6.60 ± 0.36 ef	0.070 ± 0.01 gh	0.042 ± 0.05 b	1306 ± 69.9 g
		500	8.03 ± 0.25 j	6.03 ± 0.25 f	0.066 ± 0.01 i	0.042 ± 0.05 b	1154 ± 88.6 h
		750	5.03 ± 0.45 l	3.83 ± 1.44 g	0.052 ± 0.02 k	0.041 ± 0.03 b	425 ± 21.5 j
	30	0	10.93 ± 0.11 ab	8.93 ± 0.11 ab	0.087 ± 0.05 b	0.043 ± 0.01 b	1893 ± 22.8 bc
		250	10.53 ± 0.25 bc	7.86 ± 0.92 cd	0.083 ± 0.01 cd	0.042 ± 0.01 b	1717 ± 66.2 de
		500	9.80 ± 0.20 d-f	7.83 ± 0.28 cd	0.080 ± 0.01 d	0.042 ± 0.05 b	1625 ± 53.1 e
		750	9.16 ± 0.28 f-h	7.26 ± 0.46 de	0.073 ± 0.02 fg	0.041 ± 0.01 b	1084 ± 27.8 h
Qian You No. 1	0	0	9.30 ± 0.62 e-g	7.70 ± 0.17 d	0.076 ± 0.01 ef	0.046 ± 0.05 a	1631 ± 76.1 e
		250	8.73 ± 0.32 g-i	6.73 ± 0.51 ef	0.073 ± 0.01 fg	0.046 ± 0.02 a	1422 ± 76.4 fg
		500	8.23 ± 0.20 ij	6.23 ± 0.20 f	0.069 ± 0.01 h	0.043 ± 0.05 b	1302 ± 37.4 g
		750	5.76 ± 0.68 k	3.76 ± 0.68 g	0.056 ± 0.02 j	0.041 ± 0.01 b	572 ± 36.6 i
	30	0	11.26 ± 0.25 a	9.26 ± 0.25 a	0.090 ± 0.05 a	0.046 ± 0.02 b	2053 ± 50.3 a
		250	10.73 ± 0.25 ab	8.73 ± 0.25 a-c	0.086 ± 0.01 bc	0.046 ± 0.01 b	1907 ± 49.3 b
		500	10.06 ± 0.32 cd	8.06 ± 0.32 b-d	0.083 ± 0.01 cd	0.044 ± 0.01 b	1776 ± 62.7 cd
		750	9.90 ± 0.17 c-e	7.90 ± 0.17 cd	0.076 ± 0.03 e	0.042 ± 0.05 b	1408 ± 193.9 fg

Table 2. Effect of seed priming with PEG (30%) on root and shoot length (cm), seedling fresh and dry weight (g) and seedling vigor index of two rice cultivars under different ZnO nanorods concentrations. The same letters within a column indicate there was no significant difference at a 95% probability level at the $p < 0.05$ level, respectively.

reduced under higher nano-ZnO concentration (750 mg L⁻¹) as compared to the non-stressed plants. While, the lowest leaf surface area was observed under control conditions in both cultivars. However, the reduction in leaf area was more accentuate in cultivar Zhu Liang You 06 as compared to cultivar Qian You No. 1. In contrast, the maximum mean germination time were observed under higher nano ZnO stress (750 mg L⁻¹) as compared to non-stressed plants in each cultivar. The data revealed that seed priming with PEG resulted in reduced mean germination time and significantly increased the leaf surface area in both cultivars irrespective of nano-ZnO concentrations (Table 1).

Exposure to different concentrations of nano-ZnO resulted in phenotypic changes as visualized by reductions in shoot and root lengths (Supplementary Fig. 1). As compared to control plants, significant gradual decrease in shoot and root length as well as seedling fresh and dry weight were observed in stressed plants with increasing nano-ZnO concentrations (Table 2). It was noticed that there was significant difference in shoot and root length as well as seedling fresh and dry weight at all nano-ZnO concentrations among the both cultivars. Nevertheless, the reduction in leaf area was more obvious in cultivar Zhu Liang You 06 as compared to cultivar Qian You No. 1. In addition, seed priming with PEG (30%) significantly increased the shoot and root length as well as seedling fresh and dry biomass irrespective of nano-ZnO concentrations. Similar trend was observed in case of seedling vigor index (Table 2).

Photosynthetic pigments. Results showed that nano-ZnO stress alone significantly decreased Chl a, Chl b, total Chl, and carotenoid contents as compared to control (Fig. 1). However, the reduction in Chl a, Chl b, total Chl, and carotenoid contents was more clear upon exposure to 750 mg L⁻¹ of nano-ZnO as compared to non-stressed plants. There was significant difference between the two cultivars in chlorophyll attributes under nano-ZnO concentrations. Results demonstrated that a linear decrease was observed in chlorophyll a, chlorophyll b, total chlorophyll and carotenoids contents under different nano-ZnO concentrations in two rice cultivars, this decrease was more pronounced in cultivar Zhu Liang You 06 as compared to cultivar Qian You No. 1 (Fig. 1). Seed priming with PEG significantly increased chlorophyll a (Chl a), chlorophyll b (Chl b), total chlorophyll (total Chl), and carotenoid contents under nano-ZnO stress in leaves of both rice cultivars as compared to control (Fig. 1).

Antioxidants enzyme activities and malondialdehyde contents. Under nano-ZnO stress alone, activities of antioxidant enzymes and malondialdehyde contents were differentially modulated. The present study showed that higher concentration of nano-ZnO (750 mg L⁻¹) significantly increased the activities of SOD, POD and CAT as well as enhanced the MDA contents in both cultivars as compared to non-stressed plants (Fig. 1). Interestingly, the increasing of SOD, POD, CAT activity and MDA contents was more noticeable in cultivar Zhu Liang You 06 as compared to cultivar Qian You No. 1. Taken together, priming seed with PEG (30%) resulted in a significant reduction in the levels of

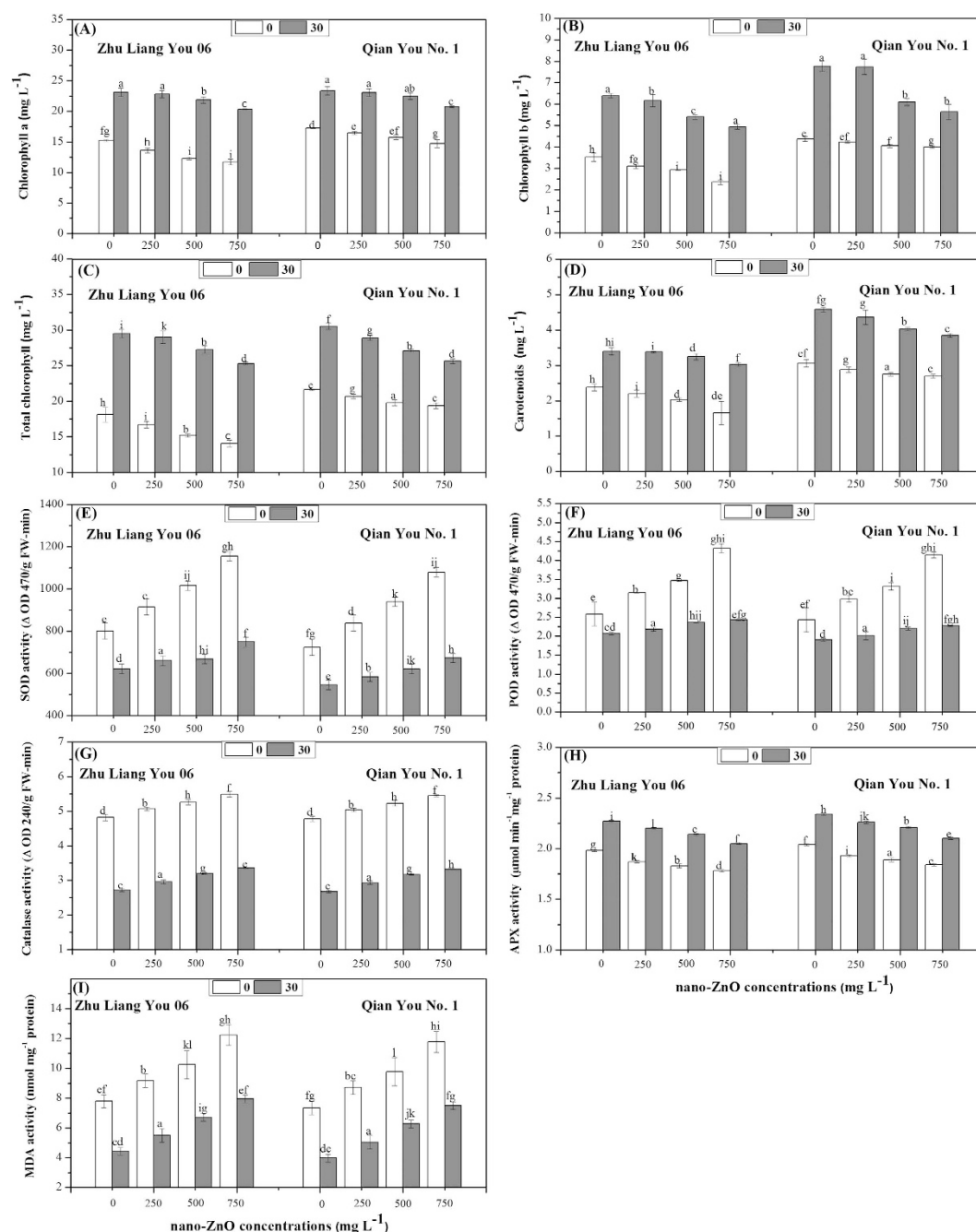


Figure 1. Effects of seed priming with PEG (30%) on (A) chlorophyll a, (B) chlorophyll b, (C) total chlorophyll, (D) carotenoids, (E) superoxide dismutase (SOD), (F) peroxidase (POD), (G) catalase (CAT), (H) ascorbate peroxidase (APX) and (I) malondialdehyde (MDA) contents in leaves of two cultivars of *Oryza sativa* under different concentrations of nano-ZnO stress.

SOD, POD, CAT activities and MDA contents at 5% probability level as compared with control plants (Fig. 1E–G,I, respectively). In contrast, the data showed that higher concentration of nano-ZnO (750 mg L⁻¹) decreased APX activity significantly in both cultivars as compared to those of non-stressed plants (Fig. 1H). However, the results showed that seed priming with PEG (30%) induced a significant increase in APX activity under different concentrations of nano-ZnO as compared to unprimed seeds and this increase in APX activity was more accentuate in cultivar Qian You No. 1 as compared to cultivar Zhu Liang You 06 irrespective of nano-ZnO concentrations (Fig. 1H).

Gene expression. There was a significant difference in *APXa* expression in both root and shoot under different nano-ZnO concentrations. Significant up-regulation of *APXa* was observed in shoots after exposure to 500 and 750 mg L⁻¹ nano-ZnO in both cultivars and the highest transcript levels of *APXa*

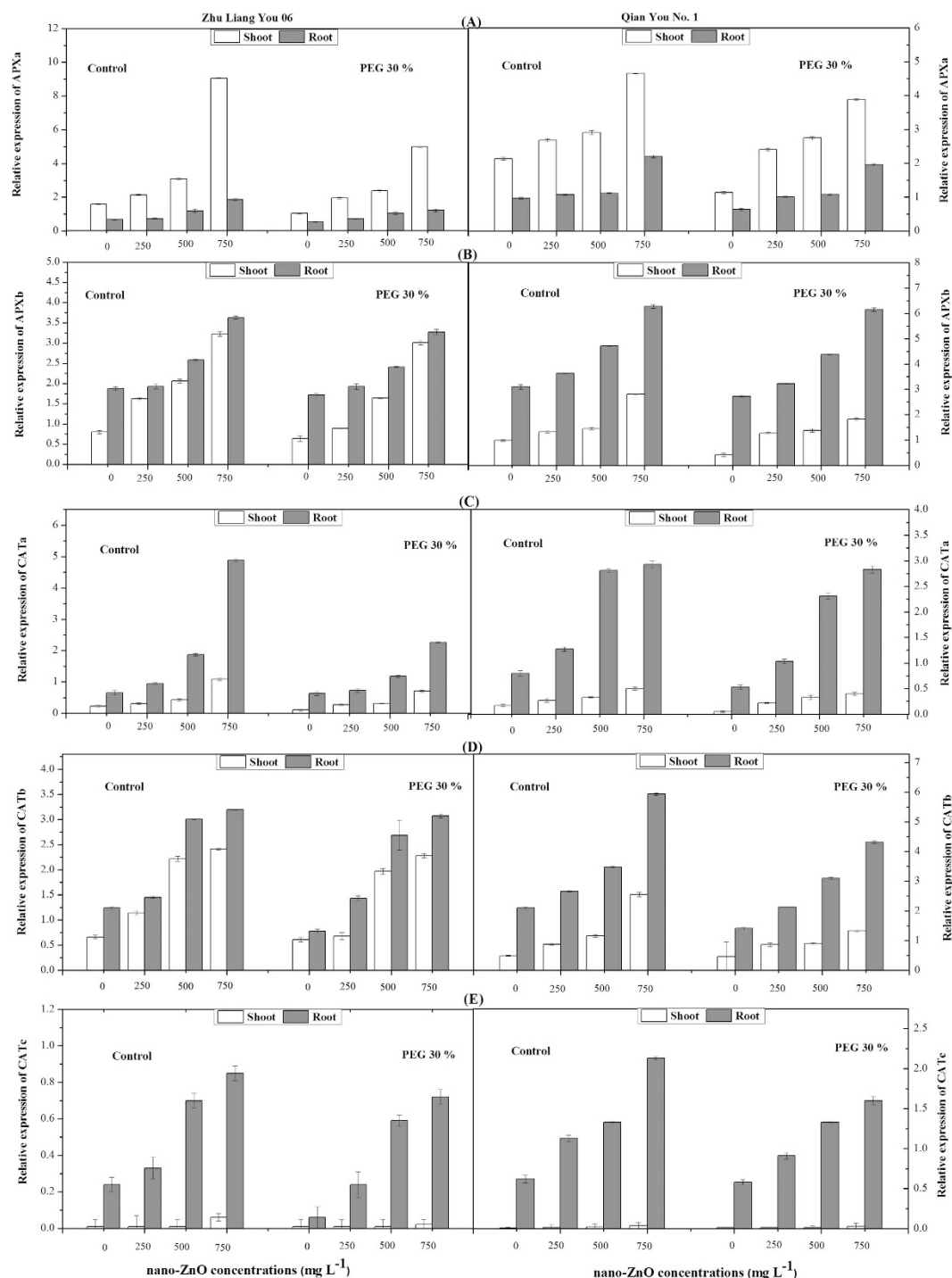


Figure 2. Effects of seed priming with PEG (30%) on gene expressions of (A) *APXa*, (B) *APXb*, (C) *CATa*, (D) *CATb* and (E) *CATc* in shoots and roots of two cultivars of *Oryza sativa* under different concentrations of nano-ZnO stress.

was observed upon exposure to 750 mg L⁻¹ as compared to non-stressed plants (Fig. 2A). Significant up-regulation of *APXa* was found in roots upon exposure to 500 and 750 mg L⁻¹ nano-ZnO in both cultivars and this increase in transcript of *APXa* was more pronounced in cultivar Qian You No. 1 as compared to cultivar Zhu Liang You 06 ($p < 0.01$) (Fig. 2A). The results indicated that seed priming with PEG (30%) induced significant reduction in transcript levels of *APXa* gene in both cultivars as compared with control (Fig. 2A). Similarly, exposure to different nano-ZnO concentrations induced a significant difference in *APXb* gene expression in both shoot and root of two cultivars. It was noticed that higher nano-ZnO concentration resulted in significant up-regulation in root and shoot of both

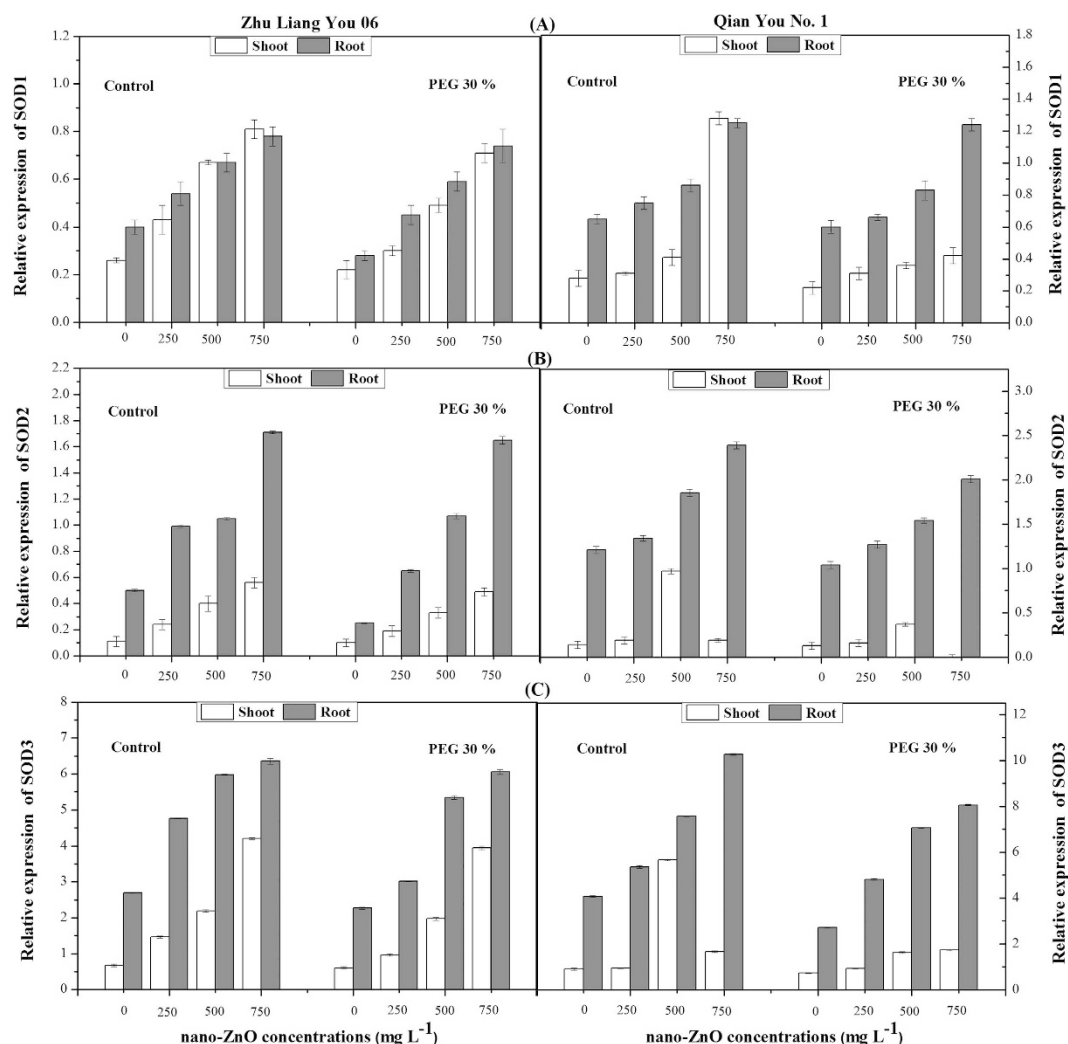


Figure 3. Effects of seed priming with PEG (30%) on gene expressions of (A) *SOD1*, (B) *SOD2* and (C) *SOD3* in shoots and roots of two cultivars of *Oryza sativa* under different concentrations of nano-ZnO stress.

cultivars (Fig. 2B). Irrespective of nano-ZnO concentrations, priming with PEG (30%) induced significant decrease in *APXb* gene expression in root and shoot of both cultivars as compared to the control (Fig. 2B).

Taken together, the data demonstrated that the highest concentrations of nano-ZnO (750 mg L⁻¹) enhanced the expression levels of *CATa*, *CATb* and *CATc* genes in root and shoot of both cultivars as compared to non-stressed conditions (Fig. 2). However, the increase in transcript levels of *CAT* genes was highly significant in root as compared to shoot in both cultivars. It was observed that the reduction was more prominent in cultivar Qian You No. 1 as compared to cultivar Zhu Liang You 06. Irrespective of nano-ZnO concentrations, seed priming with PEG (30%) induced significant reduction in transcription levels of *CATa*, *CATb* and *CATc* genes in root and shoot of both cultivars as compared to control (Fig. 2C–E).

Significant up-regulation in *SOD1* gene expression in root and shoot at all concentrations of nano-ZnO was observed (Fig. 3A). The highest expression of *SOD1* gene was observed in shoot upon exposure to 750 mg L⁻¹ in both cultivars as compared to non-stressed plants. However, seed priming with PEG significantly decreased the *SOD1* expression under nano-ZnO stress conditions in both cultivars. This reduction in transcript levels of *SOD1* gene was more clearly in root and shoot of cultivar Qian You No. 1 as compared to cultivar Zhu Liang You 06. Moreover, a significant increase in *SOD2* expression was observed with increasing nano-ZnO concentration in both cultivars. Furthermore, data showed that seed priming with PEG induced decrease in transcription level of *SOD2* in both rice cultivars as compared to control plants (Fig. 3B). Likewise, exposure to high stress of nano-ZnO induced significant up-regulation in *SOD3* gene expression in both cultivars as compared to non-stressed plants. However, the up-regulation was clearly in root as compared to shoot irrespective of nano-ZnO concentrations

(Fig. 3C). Results clearly described that seed priming with PEG induced decrease in *SOD3* gene expression in both root and shoot of two cultivars irrespective of nano-ZnO concentration (Fig. 3C).

Ultrastructural changes. The ultrastructural changes in leaf mesophyll and root tip cells under control and higher nano-ZnO concentration (750 mg L^{-1}) have been illustrated in Fig. 4. The TEM micrographs of leaf cell of cultivar Zhu Liang You 06 at control showed clean and thin cell walls, well-developed chloroplast with granule thylakoid, and the cell with rich contents and normal organelles (Fig. 4A). While, The TEM micrographs of leaf mesophyll of cultivar Zhu Liang You 06 (unprimed with PEG and exposed to 750 mg L^{-1}) are displayed in Fig. 4C. It was found that this concentration destructed the cell wall and untidy arrangement of the thylakoid inside the chloroplast as compared to their respective control. Whereas, priming with PEG reduced the stress effect represented in clear cell wall (CW), well developed chloroplast (Ch) and tidy granule thylakoid inside the chloroplast (Fig. 4B), as well as no significant changes were found in the leaf mesophyll cell among two cultivars.

The TEM micrographs of root tip cells of cultivar Zhu Liang You 06 and cultivar Qian You No. 1 of control and priming treatments are demonstrated in Fig. 4(G–L). At control level, microscopic analysis showed that root tip cells of both cultivars presented clear cell walls, the cell had normal typical oval shaped mitochondria, a large size and well developed nucleus (Fig. 4G,J). While, The TEM micrographs of root tip of both cultivars primed with PEG (30%) and exposed to 750 mg L^{-1} showed that the rough ribosome (RER) was not swollen and had rich ribosomes (Fig. 4H,K). Moreover, the cell had more vacuoles and more deposition in the vacuole, and this reaction may reduce the effect of heavy metal on the cell (Fig. 4H,K). Whereas, the TEM micrographs of root tip of both unprimed cultivars and exposed to high stress (750 mg L^{-1}) showed that the mitochondria and their cristae were swollen. The rough ribosome (RER) showed a little swollen and a part of the ribosomes was detached (Fig. 4I,L).

Discussion

The present study was carried out to highlight the effects of seed priming with 30% PEG on the physiological and molecular mechanisms of two cultivars of *Oryza sativa* under nano-ZnO stress. In the present investigation, physiological parameters in terms of germination percentage, germination index, energy of germination, mean germination time and leaf surface area per plant significantly decreased with increasing nano-ZnO concentrations (Table 1). Recently, Lin and Xing investigated the effect of NPS in several physiological experiments and revealed that the phytotoxic dose of nanoparticles (NPs) varies between species under investigation. Furthermore, percent inhibitory concentrations (IC_{50}) of nano-Zn and nano-ZnO were estimated to be near 50 mg L^{-1} for radish, and about 20 mg L^{-1} for rape and ryegrass⁷. The present study suggested that improvement of germination characters in primed seeds could be linked to physiological effects of pre-treatment. Indeed, primed seeds exhibited a faster imbibition as compared to unprimed seeds. In this trend, Nagarajan *et al.* also reported that improvement of germination by priming with PEG might be directly related to the modification of seed water relations¹⁷. Furthermore, this study therefore suggested that vacuums created inside the seed as a result of priming made water flow easier, thus contributing to tissue hydration. Additionally, Nagarajan *et al.* hypothesized that better performance of primed tomato seeds may be attributed to modifications of seed water binding properties during imbibition¹⁷. In this regard, Shaw and Hossain reported a significant inhibition in rice seed germination exposed to 0.5 mM nano-CuO treatment¹⁸. Nevertheless, Shaw *et al.* showed that nano-copper stress had no apparent effects on seeds germination of barley¹⁹.

The data further depicted a decreasing trend in seedling dry and fresh weight with increasing nano-ZnO concentrations (Table 2). According to the results, it was found that nano-ZnO stress caused significant toxic effects on the morphological characteristics of *Oryza sativa* as compared to non-stressed plants. A significant decrease in growth was found and this might be due to the adverse effects of nano-ZnO stress on the roots so the plants were not able to take up nutrients and continue their normal activity. Several study indicated that heavy metals stress induced a decrease in fresh and dry biomass which can inhibit the photosynthetic electron transport chain and ultimately result in biomass reduction²⁰. Moreover, inhibition of plant biomass might be due to inhibition of photosynthesis, inactivity of both photosystem II and the enzymes of carbon reduction cycles¹⁰.

In present study, a significant reduction in chlorophyll attributes and carotenoids contents was observed in *Oryza sativa* seedlings exposed to nano-ZnO stress (Fig. 1A–D). The significant reduction in chlorophyll attributes, as observed in this study, might be due to the reduced biomass or as a result of excess lipid peroxidation of chloroplast membranes due to oxidative stress²¹. Similarly, significant reduction in chlorophyll attributes as a result of silver nanoparticles (AgNPs) exposure had also been reported from *Spirodela polyrhiza*²² and *Arabidopsis thaliana*²¹. Moreover, significant reduction in total carotenoids content upon exposure to AgNPs and may negatively affect the plants ability to quench excess ROS²³.

Data regarding the antioxidant enzyme activities showed that SOD activity was increased in rice plants growing under toxic levels of nano-ZnO stress (Fig. 1E). Increase in SOD activity in response to stress appeared to be probably due to de-novo synthesis of the enzyme protein²⁴. SOD activity has been reported to increase under salinity²⁵ and heavy metals toxicity²⁶. The present study indicated an enhancement in POD activity under nano-ZnO stress (Fig. 1F) which suggested that this enzyme served as an intrinsic defense tool to resist ZnO induced oxidative damage in rice plants. Under salinity and metal toxicity conditions, the level of POD had been used as potential biomarker to evaluate the intensity

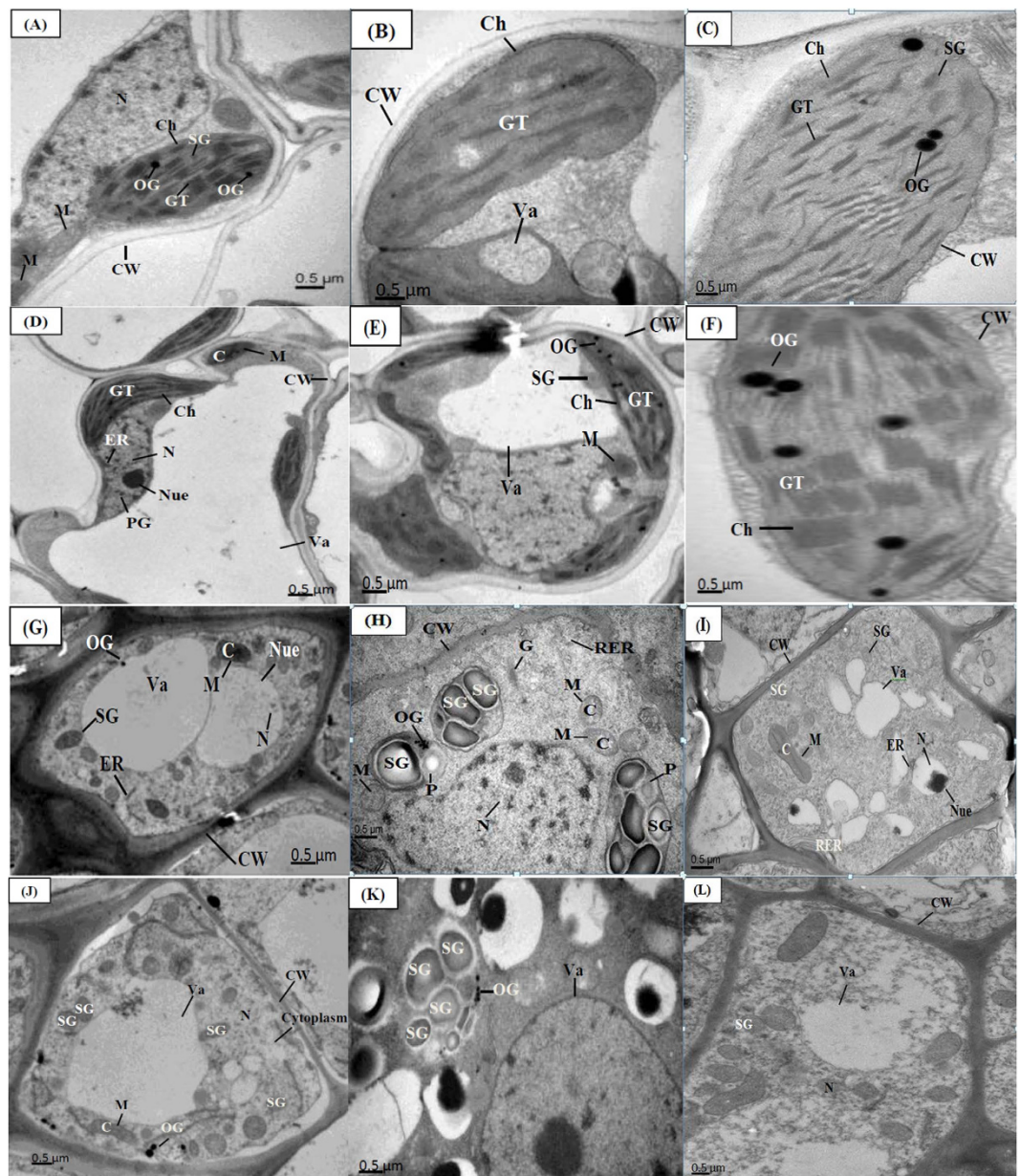


Figure 4. Electron micrographs of leaf mesophyll and root cell of two cultivars of *Oryza sativa* (cvs. Zhu Liang You 06 and Qian You No. 1) primed with PEG (30%) and grow under control and 750 mg L⁻¹ of nano-ZnO concentration. (A) Leaf mesophyll cell of cultivar Zhu Liang You 06 at control level. (B) Leaf mesophyll cell of cultivar Zhu Liang You 06 primed with PEG (30%) and exposed to 750 mg L⁻¹. (C) Leaf cell of cultivar Zhu Liang You 06 non-primed with PEG and exposed to 750 mg L⁻¹. (D) Leaf mesophyll cell of cultivar Qian You No. 1 under control. (E) Leaf mesophyll cell of Qian You No. 1 primed with PEG (30%) and exposed to 750 mg L⁻¹. (F) Leaf mesophyll cell of Qian You No. 1 non-primed with PEG (30%) and exposed to 750 mg L⁻¹. (G) Root tip of cultivar Zhu Liang You 06 under control. (H) Root tip of cultivar Zhu Liang You 06 primed with PEG (30%) and exposed to 750 mg L⁻¹. (I) Root tip of cultivar Zhu Liang You 06 non-primed with PEG (30%) and exposed to 750 mg L⁻¹. (J) Root tip of cultivar Qian You No. 1 under control. (K) Root tip of cultivar Qian You No. 1 primed with PEG (30%) and exposed to 750 mg L⁻¹. (L) Root tip of cultivar Qian You No. 1 non-primed with PEG and exposed to 750 mg L⁻¹.

of stress²⁶. Increased POD activity has been documented under a variety of stressful conditions such as water stress²⁷, salinity²⁸ and toxic levels of Al, Cu, Cd, Zn²⁶. Moreover, increased POD activity in Pb-stressed seedlings might be due to increased release of peroxidases localized in the cell walls²⁹.

Results showed that CAT activity was significantly enhanced under different nano-ZnO concentrations i.e. 500 and 750 mg L⁻¹. While, APX activity decreased in relation to different nano-ZnO concentrations (Fig. 1G,H). The increase of CAT activity in leaves under nano-ZnO stress suggested that its

effective scavenging mechanism to remove H_2O_2 resulted from metal stress caused oxidative damage³⁰. However, reduction in antioxidant enzyme activities might be due to the oxidative stress, inhibition of enzyme synthesis and change in the assemblage of enzyme subunits³¹.

The MDA content is often measured as a suitable physiological index to reflect the degree of lipid peroxidation (MDA) and stress tolerance in plants³². Change in MDA concentration has been used as a parameter to assess oxidative stress damages to lipid membranes³³. In the present study, MDA contents were enhanced in both cultivars under nano-ZnO stress. However, seed priming with PEG decreased MDA contents under different concentrations of nano-ZnO (Fig. 11). These results are in consistent with the observations, showing that ALA could attenuate abiotic stress, probably due to its ability to act as antioxidant scavenging ROS³⁴.

Gene expression in response to heavy metals stress is usually studied at the level of mRNA abundance because this gives a more precise estimate of antioxidant gene activation than enzyme activity. For this reason, we studied multiple components of the antioxidant enzymes at both the enzymatic and transcriptional level. Expression of *APX* genes had been demonstrated to be enhanced in plants by NaCl treatment³⁵. In agreement with our results, Gupta *et al.* reported that *APX* transcripts might be up-regulated by increased levels of H_2O_2 in tobacco chloroplasts as results of Cu-Zn-superoxide dismutase overexpression³⁶. Further, it was also found that catalase genes (*CATa*, *CATb* and *CATc*) were significantly enhanced in both root and shoot under different concentrations of nano-ZnO (Fig. 2C–E). Significant increase in catalase transcription, despite no significant change was observed in catalase enzymatic activity of leaves of *Arabidopsis thaliana*³⁷. These discrepancies can be due to the presence of multiple allo- or isozymes. Alternatively, nano-ZnO stress could cause an enhanced break down of the proteins, which in turn also leads to an enhanced transcription. In the present study, it was observed that the expression levels of different *SOD* genes (*SOD1*, *SOD2* and *SOD3*) also showed significant induction upon exposure to different concentrations of nano-ZnO (Fig. 3A–C) showing that oxidative stress caused in different cellular compartments of the cell as a result of nano-ZnO exposure. In general, high significant changes in the transcript level of most antioxidative genes were found, but not all genes showed similar responses in roots and shoots. Most of genes were significantly up-regulated in root as compared to shoots that may be due to that plant roots are the first point of contact for these toxic of nano-ZnO. These observations supported the view of Smeets *et al.* who indicated that the underlying mechanism of oxidative stress was different in the roots and leaves. Additionally, the generation of superoxide and the lipoxygenase activity are the main causes of oxidative stress in the roots, whereas in the leaves H_2O_2 seemed to be an important candidate. Whether, this H_2O_2 was produced locally as a result of increased Cd content of the leaves, or whether it arrived as a signal from the roots, remains to be elucidated³⁷.

In the present study, the ultrastructural changes occurred in different parts of plant cells were found to be dose-dependent. The leaf mesophyll cells were significantly damaged at 750 mg L^{-1} nano-ZnO in both cultivars, however the damage was prominent in cultivar Zhu Liang You 06 as compared to cultivar Qian You No. 1 (Fig. 4A–F). The number of osmiumphobic granule and starch grains increased in leaf cells in both cultivars under nano-ZnO stress which indicated that plants might undergo in stress under metal stress³⁰. The root tip cells of cultivar Zhu Liang You No. 1 were significantly damaged under nano-ZnO stress as compared to cultivar Qian You No. 1. The disappearance of different organelles and ruptured cell structure was found in cultivar Zhu Liang You 06 under nano-ZnO stress (Fig. 4L). Previous study showed that heavy metal toxicity damaged the root tip cells of *Brassica napus*³⁸. Moreover, Daud *et al.* observed the presence of plasmolysis in root tips cells of cotton under the different concentrations of Cd³⁹. However, seed priming with PEG significantly improved the cellular ultrastructure of leaf and root in both rice cultivars under nano-ZnO stress conditions (Fig. 4B,E,H,K). Cell structure was improved when citric acid applied with Cd-treated plants in *Juncus effusus*⁴⁰. Thus, it could be concluded that seed priming with PEG (30%) could decrease antioxidant enzymes activities, leading to avoid cell ultrastructure damage.

In summary, the exposure of rice seeds to nano-ZnO had a clear phytotoxic effect on the physiological, antioxidant enzymes and molecular mechanism of rice seedlings. Data suggested that seed priming with PEG (30%) alleviated the toxicity of nano-ZnO to *Oryza sativa* seeds and improved both germination and early seedling growth under different concentrations of nano-ZnO. Moreover, this study depicted that Qian You No. 1 proved to be more resistant to nano-ZnO stress as compared to Zhu Liang You 06 cultivar. The electron microscopic study revealed that ruptured cell in leaf and root tip were more prominent in Zhu Liang You 06 as compared to Qian You No. 1 cultivar under control and high stressed plants.

Methods

Engineered ZnO nanorods. Dispersions of nanorods used in this study were prepared at the laboratory of the Center of Nanotechnology, College of Agriculture and Biotechnology, Zhejiang University, China. Zinc oxide nanorods (nano-ZnO) were prepared from commercial ZnO nanopowder (Sigma-Aldrich, USA) by dispersing nanorods in Milli-Q water through ultrasonication (300 W, 40 kHz) for 30 min. The TEM Images of ZnO nanorods were taken by using scion image processing software (Fig. 5A). Average zeta potential of nano-ZnO in water and nano-ZnO in PEG was measured by Zetasizer nano (Zs3590, Malvern, United Kingdom) (Fig. 5B). The average length and diameter of the ZnO nanorods were 0.25 nm and 117 nm respectively, measured by Nano Measured software (Fig. 5C,D).

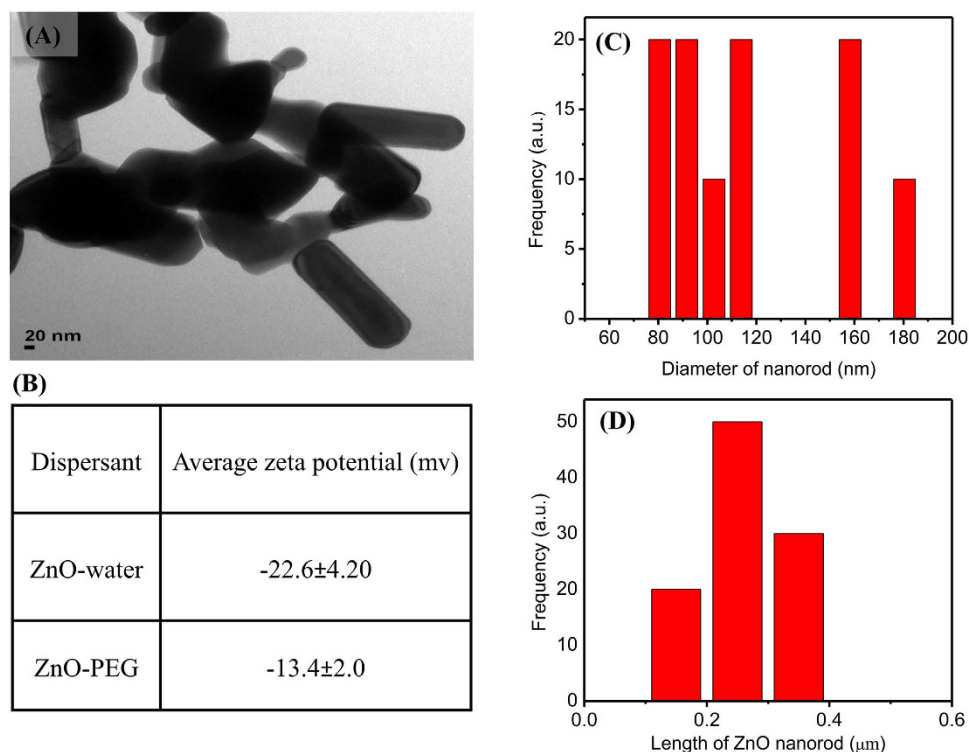


Figure 5. (A) Transmission electron microscopy (TEM) after dispersed in Milli-Q water of nano-ZnO scale 20 nm. (B) Average zeta potential of nano-ZnO in water and nano-ZnO in PEG. (C) Diameter of ZnO nanorod (nm). (D) Length of ZnO nanorod (μm).

Plant material and growth conditions. Seeds of two cultivars of *Oryza sativa*, L. (cvs. Zhu Liang You 06 and Qian You No. 1) were obtained from the Center of Seed Science, College of Agriculture and Biotechnology, Zhejiang University, China. The seeds were surface sterilized with 0.5% NaClO solution for 15 min and then washed several times with tap water followed by washing with sterilized distilled water for thrice to remove the traces of the disinfectant. The sterilized seeds were primed at 15°C in darkness for 24 hr with PEG 30%. Then, seeds were dried back to their original moisture contents at room temperature. The unprimed dry seeds were used as control (CK). After priming, seed germination tests were carried out. Fifty seeds for each treatment were placed in a plastic germination box (12 cm × 18 cm) and each treatment replicated three times. Then, seeds were incubated in a germination chamber at 25°C under alternating cycle of 8 hr illumination and 16 hr darkness for 14 days⁴¹. The incubated seeds were exposed to different concentrations of nano-ZnO (NPs ≤ 100 nm) i.e. 0, 250, 500 and 750 mgL⁻¹. The nano-ZnO concentrations were based on findings from preliminary studies. Nano-ZnO at 250 mgL⁻¹ concentration showed a little damage to plant growth. While, nano-ZnO at 750 mgL⁻¹ concentration imposed a significant damage to plant growth. Whereas, concentrations higher than 750 mgL⁻¹ were too toxic for plant growth. Furthermore, ZnO nanorods size was determined based on the pre-experiment study. It was clearly observed that ZnO nanorods larger than 100 nm showed a greater level of inhibition of seed germination and seedling growth. For this reason, only NPs ≤ 100 nm of ZnO were used.

Physiological parameters. The germinated seeds were counted daily for 14 days. Then, the germination percentage was calculated at the 14th Day. The germination index and mean germination time were calculated as the following equation⁴²:

$$GI = \sum (G_t/T_t) \text{ and } MGT = \sum (G_t \times T_t) / \sum G_t \quad (1)$$

where G_t is the number of germinated seeds on Day t , T_t is time corresponding to G_t in days. Energy of germination was calculated as the percentage of germinating seeds at the 4th day after sowing relative to the number of seeds tested⁴³. For seedling parameter measurements, fourteen day old seedlings were harvested, the length of shoots and roots, and the leaf area of randomly selected ten plants per treatment were measured manually. Dry and fresh weight of the rice seedlings was determined separately. Fresh weight of ten seedlings per treatment were weighed immediately after harvesting and then placed into an oven at 80°C for 24 hr. The dried samples were weighed immediately after removal from the oven until the weight became stable⁴⁴. For RNA extraction, until their respective analysis. Seedling vigor the control

and nano-ZnO exposed seedlings, frozen in liquid nitrogen and stored at -80°C until their respective analysis. Seedling vigor index was calculated as the following formula⁴⁵:

$$\text{VI} = \text{Germination (\%)} \times [\text{Shoot length (cm)} + \text{Root length (cm)}]. \quad (2)$$

Photosynthetic pigments determination. The amount of photosynthetic pigments in terms of chlorophyll a, chlorophyll b, total chlorophyll and carotenoids were determined according to the method of Hartmut *et al.* In brief, Fresh leaf tissues (0.2 g) was homogenized in 3 mL ethanol (95%, v/v). The homogenate was centrifuged at 5000 g for 10 min and the supernatant was extracted. Then, 9 mL ethanol (95%, v/v) was added to 1 mL aliquot of the supernatant. After that, the mixture was determined by monitoring the absorbance at the wavelengths 665, 649, and 470 nm by using spectrophotometer⁴⁶. The following equations were used for the calculation of pigment amounts:

$$\text{Chlorophyll a (C}_a\text{)} = 13.95 A_{665} - 6.88 A_{649} \quad (3)$$

$$\text{Chlorophyll b (C}_b\text{)} = 24.96 A_{649} - 7.32 A_{665} \quad (4)$$

$$\text{Carotenoids (C}_{x+c}\text{)} = (1000 A_{470} - 2.05 C_a - 104 C_b) / 245 \quad (5)$$

$$\text{Total chlorophyll content} = C_a + C_b \quad (6)$$

The amounts of pigments were calculated as milligrams per litre of plant extract.

Antioxidant enzyme activities and malondialdehyde contents. In order to measure the anti-oxidant enzyme activities (SOD, CAT, APX and POD) and malondialdehyde (MDA) contents, leaf samples (0.5 g) were taken per treatment and homogenized in 8 mL of 50 mM potassium phosphate buffer (pH 7.8) under ice cold conditions. Homogenate was centrifuged at 10,000 g for 20 min at 4°C and the supernatant was used for the determination of the following enzyme activities. Superoxide dismutase (SOD) activity was assayed by measuring its ability to inhibit the photochemical reduction of nitroblue tetrazolium (NBT)⁴⁷. NBT reaction solution contained 50 mmol L^{-1} phosphate buffer (pH 7.8), 13 mmol L^{-1} methionine, 75 $\mu\text{mol L}^{-1}$ NBT, 2 $\mu\text{mol L}^{-1}$ riboflavin, 0.1 mmol L^{-1} EDTA. The reaction mixture was 3.1 mL, which contained 3 mL NBT reaction solution and 0.1 mL of enzyme extract. Reaction was started by adding 2 $\mu\text{mol L}^{-1}$ riboflavin and placing the reaction tubes under 15 W fluorescent lamps for 15 min. A complete reaction mixture without enzyme extract served as a control. The photo reduction of NBT was measured at 560 nm and one unit of SOD was defined as being present in the volume of extract that caused inhibition of the photo- reduction of NBT by 50%. Guaiacol peroxidase (POD) activity was measured with guaiacol as the substrate in a total volume of 3 mL⁴⁸. The 3 mL reaction mixture consisted of 2.7 mL phosphate buffer (25 mM, pH 7.0), 0.1 mL guaiacol (1.5%), 0.1 mL H_2O_2 (0.4%) and 0.1 mL of enzyme extract. Increase in the absorbance due to oxidation of guaiacol ($E = 25.5 \text{ mM}^{-1} \text{ cm}^{-1}$) was measured at 470 nm. The enzyme activity was calculated in terms of l M of guaiacol oxidized $\text{g}^{-1} \text{ FW min}^{-1}$ at $25 \pm 2^{\circ}\text{C}$.

Catalase (CAT) activity was measured by reduction in absorbance at 240 nm due to the decline of extinction H_2O_2 . The 3 mL reaction mixture containing 2.8 mL phosphate buffer (25 mM, pH 7.0), 0.1 mL H_2O_2 (0.4%) and 0.1 mL enzyme extract was used. The reaction was started with the addition of H_2O_2 ⁴⁹. The enzyme activity was calculated in terms of l M of H_2O_2 $\text{g}^{-1} \text{ FW min}^{-1}$ at $25 \pm 2^{\circ}\text{C}$. Ascorbate peroxidase (APX) activity was measured according to⁵⁰. The assay depended on the decrease in absorbance at 290 nm as ascorbate was oxidized. The 3 mL reaction mixture consisted of 2.7 mL phosphate buffer (25 mM, pH 7.0), 0.1 mL ascorbate (7.5 mM), 0.1 mL H_2O_2 (0.4%) and 0.1 mL of enzyme extract. The reaction started by addition of H_2O_2 . The enzyme activity was calculated in terms of ($\mu\text{mol min}^{-1} \text{ mg}^{-1}$ protein) at $25 \pm 2^{\circ}\text{C}$.

Malondialdehyde (MDA) concentration was determined as 2-thiobarbituric acid (TBA) reactive metabolites²⁰. About 1.5 mL extract was homogenized in 2.5 mL of 5% TBA made in 5% trichloroacetic acid (TCA). The mixture was heated at 95°C for 15 min, and then quickly cooled on ice. After centrifugation at 5,000 g for 10 min, the absorbance of the supernatant was measured at 532 nm. Correction of nonspecific turbidity was made by subtracting the absorbance value measured at 600 nm. The concentration of MDA was calculated in terms of (nmol mg^{-1} protein).

Analysis of gene expression. Frozen leaf tissue (100 mg) was grinded thoroughly in liquid nitrogen using a pestle and mortar. Total RNA was isolated from the shoot and roots at Ck, 250, 500 and 750 mgL^{-1} of nano-ZnO stressed seedlings by using RNA isolation (Takara, Japan) following the manufacturer's instructions. The concentration of the RNA was determined by NanoDrop 2000/2000c (Thermo Scientific, USA). The RNA purity was also checked spectrophotometrically by means of the

260/280 nm ratio. The primers for *APXa*, *APXb*, *CATa*, *CATb*, *CATc*, *SOD1*, *SOD2*, *SOD3* and *ACT1* genes were designed using online NCBI Primer-blast (http://www.ncbi.nlm.gov/tools/primer-blast/index.cgi?link_LOC=BlastHome). cDNA was synthesized using Primer Script RT reagent Kit (Takara, Japan) from 1 µg of total RNA in a 20 µL reaction, and diluted 4-fold with water.

Quantitative real-time RT-PCR was performed using SYBR premix EX Taq (Takara, Japan). *ACT1* was used as an endogenous control gene to normalize expression of the other genes. Primers used in real-time RT-PCR were shown in supplementary Table 1. The PCR program was as follows: 30 s at 95 °C, followed by 40 cycles of 10 s at 95 °C, 30 s at 60 °C.

Transmission electron microscopy study. After 14 days of treatment, leaf segments without veins and root tips (8–10 each per treatment) were collected from randomly selected seedlings and then fixed overnight in 2.5% glutaraldehyde (v/v) in 0.1 M PBS (sodium phosphate buffer, pH 7.4) and washed three times with the same PBS. Then the samples were post fixed in 1% OsO₄ [osmium (VIII) oxide] for 1 hr. and washed three times in 0.1 M PBS (pH 7.4), with 10-min intervals between each washing. Then, with 15–20 min intervals, the samples were dehydrated in a graded series of ethanol (50%, 60%, 70%, 80%, 90%, 95% and 100%) and at the end washed by absolute acetone for 20 min. The samples were then infiltrated and embedded in Spurr's resin overnight. After heating at 70 °C for 9 hr, ultrathin sections (80 nm) of specimens were prepared and mounted on copper grids for viewing by a transmission electron microscope (JEOLTEM- 1230EX) at an accelerating voltage of 60.0 kV.

Statistical analysis. Treatments were arranged in factorial experimental in completely randomized design. All values described in results section were mean of three replications \pm standard deviation (SD). Percentage data were arcsin-transformed before analysis according to $\hat{y} = \arcsin [\sqrt{x/100}]$. The data were analyzed using SPSS v16.0 (SPSS, Inc., Chicago, IL, USA). Analysis of variance (ANOVA) was carried out, followed by Duncan's multiple range test between the means of treatments to determine the significant difference at the $p < 0.05$ and 0.01 level between mean values.

References

- Sharma, S. S. & Dietz, K. J. The relationship between metal toxicity and cellular redox imbalance. *Trends Plant Sci.* **14**, 43–50 (2009).
- Dietz, K. J. & Herth, S. Plant nanotoxicology. *Trends Plant Sci.* **16**, 582–589 (2011).
- Castiglione, M. R., Giorgetti, L., Geri, C. & Cremonini, R. The effects of nano-TiO₂ on seed germination, development and mitosis of root tip cells of *Vicia narbonensis*, L. and *Zea mays*, L. *J. Nanopart. Res.* **13**, 2443–2449 (2011).
- Boonyanitpong, P., Kositsup, B., Kumar, P., Baruah, S. & Dutta, J. Toxicity of ZnO and TiO₂ nanoparticles on germinating rice seed *Oryza sativa*, L. *Int. J. Biosci. Biochem. Bioinf* **1**, 282–285 (2011).
- Ng, K. W. The role of the tumor suppressor p53 pathway in the cellular DNA damage response to zinc oxide nanoparticles. *Biomaterials*. **32**, 8218–8225 (2011).
- Giovanni, M. et al. Toxicity profiling of water contextual zinc oxide, silver, and titanium dioxide nanoparticles in human oral and gastrointestinal cell systems. *Environ. Toxicol.* **10**, 1–11 (2015).
- Lin, D. & Xing, B. Phytotoxicity of nanoparticles: inhibition of seed germination and root growth. *Environ. Pollut.* **150**, 243–250 (2007).
- Breckle, S. W., Waisel, Y., Eshel, A. & Kafkafi, X. *Growth under stress, heavy metals: Plant roots*. [351–373] (Marcel Dekker New York, 1991).
- Chia, S. L., Tay, C. Y., Setyawati, M. I. & Leong, D. T. Biomimicry 3D Gastrointestinal Spheroid Platform for the Assessment of Toxicity and Inflammatory Effects of Zinc Oxide Nanoparticles. *Small*. **11**, 702–712 (2015).
- Kabata-Pendias, A. & Pendias, H. *Trace Metals in Soils and Plants*. [11–12] (CRC Boca Raton, Florida, 2010).
- Hu, J., Zhu, Z. Y., Song, W. J., Wang, J. C. & Hu, W. M. Effect of sand priming on germination and field performance in direct-sown rice (*Oryza sativa* L.). *Seed Sci. & Technol.* **33**, 243–248 (2005).
- Sen, A. & Alikamanoglu, S. Antioxidant enzyme activities, malondialdehyde and total phenolic content of PEG-induced hyperhydric leaves in sugar beet tissue culture. *In Vitro Cell. Dev. Biol. Plant.* **49**, 396–404 (2013).
- Dursun, A. & Ekinici, M. Effects of different priming treatments and priming durations on germination percentage of parsley (*Petroselinum crispum* L.) seeds. *Agr. Sci.* **1**, 17–23 (2010).
- Munir, N. & Aftab, F. The role of polyethylene glycol (PEG) pretreatment in improving sugarcane's salt (NaCl) tolerance. *Turk. J. Bot.* **33**, 407–415 (2009).
- Dong, X., Bi, H., Wu, G. & Ai, X. Drought-induced chilling tolerance in cucumber involves membrane stabilisation improved by antioxidant system. *Int. J. Plant Prod.* **7**, 67–80 (2013).
- Christianson, D. W. Structural biology of zinc. *Adv. Protein Chem.* **42**, 281–295 (1991).
- Nagarajan, S., Pandita, V. K., Joshi, D. K., Sinha, J. P. & Modi, B. S. Characterization of water status in primed seeds of tomato (*Lycopersicon esculentum* Mill.) by sorption properties and NMR relaxation times. *Seed Sci. Res.* **15**, 99–111 (2005).
- Shaw, A. K. & Hossain, Z. Impact of nano-CuO stress on rice (*Oryza sativa* L.) seedlings. *Chemosphere*. **93**, 906–915 (2013).
- Shaw, A. K. et al. Nano-CuO stress induced modulation of antioxidative defense and photosynthetic performance of Syrian barley (*Hordeum vulgare* L.). *Environ. Exp. Bot.* **102**, 37–47 (2014).
- Mohanty, N., Vass, I. & Demeter, S. Impairment of photosystem II activity at the level of secondary quinone acceptor in chloroplasts treated with cobalt, nickel and zinc ions. *Physiol. Plant.* **76**, 386–390 (1989).
- Ma, C. et al. Physiological and molecular response of *Arabidopsis thaliana* (L.) to nanoparticle cerium and indium oxide exposure. *ACS Sustain. Chem. Eng.* **1**, 768–778 (2013).
- Jiang, H. S., Li, M., Chang, F. Y., Li, W. & Yin, L. Y. Physiological analysis of silver nanoparticles and AgNO₃ toxicity to *Spirodela polyrrhiza*. *Environ. Sci. Technol.* **31**, 1880–86 (2012).
- Sharma, P. K. & Hall, D. O. Interaction of salt stress and photo inhibition on photosynthesis in barley and sorghum. *J. Plant Physiol.* **138**, 614–619 (1991).
- Lozano, R., Azcon, R. & Palma, J. M. SOD and drought stress in *Lactuca sativa*, *New Phytol.* **136**, 329–331 (1996).

25. Comba, M. E., Benavides, M. P. & Tomaro, M. L. Effect of salt stress on antioxidant defence system in soybean root nodules. *Aust. J. Plant Physiol.* **25**, 665–671 (1998).
26. Shah, K., Kumar, R. G., Verma, S. & Dubey, R. S. Effect of cadmium on lipid peroxidation, superoxide anion generation and activities of antioxidant enzymes in growing rice seedlings. *Plant Sci.* **161**, 1135–1144 (2001).
27. Zhang, J. & Kirkham, M. B. Drought-stress induced changes in activities of superoxide dismutase, catalase and peroxidase in wheat species. *Plant Cell Physiol.* **35**, 785–91 (1994).
28. Mittal, R. & Dubey, R. S. Behaviour of peroxidases in rice changes in enzyme activity and isoforms in relation to salt tolerance. *Plant Physiol. Biochem.* **29**, 31–40 (1991).
29. Shalini, V. & Dubey, R. S. Lead toxicity induces lipid peroxidation and alters the activities of antioxidant enzymes in growing rice plants. *Plant Sci.* **164**, 645–655 (2003).
30. Reddy, A. M., Kumar, S. G., Jyothsnakumari, J., Thimmanaik, S. & Sudhakar, C. Lead induced changes in antioxidant metabolism of horsegram (*Macrotyloma uniflorum* (Lam.) Verdc.) and bengalgram (*Cicer arietinum* L.). *Chemosphere.* **60**, 97–104 (2005).
31. Garnier, L. *et al.* Cadmium affects tobacco cells by a series of three waves of reactive oxygen species that contribute to cytotoxicity. *Plant Cell Environ.* **29**, 1956–1969 (2006).
32. Cheng, F. Y., Hsu, S. Y. & Kao, C. H. Nitric oxide counteracts the senescence of detached rice leaves induced by dehydration and polyethylene glycol but not by sorbitol. *Plant Growth Regul.* **38**, 265–272 (2002).
33. Hossain, Z., Lopez-Climent, M. F., Arbona, V., Perez-Clemente, R. M. & Gomez-Cadenas, A. Modulation of the antioxidant system in Citrus under water logging and subsequent drainage. *J. Plant Physiol.* **166**, 1391–1404 (2009).
34. Ali, B. *et al.* 5-Aminolevulinic acid ameliorates the growth, photosynthetic gas exchange capacity, and ultrastructural changes under cadmium stress in *Brassica napus* L. *J. Plant Growth Regul.* **32**, 604–614 (2013).
35. Kawasaki, S. *et al.* Gene expression profiles during the initial phase of salt stress in rice. *Plant Cell.* **13**, 889–905 (2001).
36. Gupta, A. S., Webb, R. P., Holaday, A. S. & Allen, R. D. Overexpression of superoxide dismutase protects plants from oxidative stress. Induction of ascorbate peroxidase in superoxide dismutase-overexpression plants. *Plant Physiol.* **103**, 1067–1073 (1993).
37. Smeets, K. *et al.* Cadmium-induced transcriptional and enzymatic alterations related to oxidative stress. *Environ. Exp. Bot.* **63**, 1–8 (2008).
38. Ali, B. *et al.* Physiological and ultra-structural changes in *Brassica napus* seedlings induced by cadmium stress. *Biol. Plant.* **58**, 131–138 (2014).
39. Daud, M. K. *et al.* Cadmium-induced functional and ultrastructural alterations in roots of two transgenic cotton cultivars. *J. Hazard. Mater.* **161**, 463–473 (2009).
40. Najeeb, U. *et al.* Insight into cadmium induced physiological and ultra-structural disorders in *Juncus effusus* L. and its remediation through exogenous citric acid. *J. Hazard. Mater.* **186**, 565–574 (2011).
41. Zheng, Y. Y., Hu, J., Zhang, S., Gao, C. H. & Song, W. J. Identification of chilling tolerance in maize inbred lines at germination and seedling growth stages. *Journal of Zhejiang University (Agri. & Life Sci.)* **32**, 41–45 (2006).
42. Zhang, S., Hu, J., Zhang, Y., Xie, X. J. & Allen, K. Seed priming with brassinolide improves lucerne (*Medicago sativa*, L.) seed germination and seedling growth in relation to physiological changes under salinity stress. *Aust. J. Exp. Agric.* **58**, 811–815 (2007).
43. Ruan, S., Xue, Q. & Tylkowska, K. The Influence of Priming on Germination of Rice (*Oryza sativa*, L.) seeds and seedling Emergence and Performance in Flooded Soils. *Seed Sci. Technol.* **30**, 61–67 (2002).
44. Momoh, E. & Zhou, W. Growth and yield responses to plant density and stage of transplanting in winter oilseed rape (*Brassica napus*, L.). *J. Agron. Crop Sci.* **186**, 253–259 (2001).
45. Abdul-baki, A. A. & Anderson, J. D. Vigor determination in soybean by multiple criteria. *Crop Sci.* **13**, 630–633 (1973).
46. Hartmut, K., Lichtenthaler, A. & Welburn, R. Determinations of total carotenoids and chlorophylls a and b of leaf extracts in different solvents. *Biochem. Soc. Trans.* **11**, 591–592 (1983).
47. Rao, K. V.M. & Sresty, T. V. S. Antioxidant parameters in the seedlings of pigeon pea (*Cajanus cajan*, (L.) Millsapugh) in response to Zn and Ni stresses. *Plant Sci.* **157**, 113–128 (2000).
48. Zhang, X. Z. (ed). *The measurement and mechanism of lipid peroxidation and SOD, POD and CAT activities in biological system.* [208–211] (Research methodology of crop physiology. Agriculture Press, Beijing, 1992).
49. Cakmak, I. & Marschner, H. Magnesium deficiency and high light intensity enhance activities of superoxide dismutase, ascorbate peroxidase and glutathione reductase in bean leaves. *Plant Physiol.* **98**, 1222–1227 (1992).
50. Nakano, Y. & Asada, K. Hydrogen peroxide is scavenged by ascorbate specific peroxidase in spinach chloroplast. *Plant Cell Physiol.* **22**, 867–880 (1981).

Acknowledgements

This research was supported by the Special Fund for Agro-scientific Research in the Public Interest (No. 201203052), the National Natural Science Fund (No. 31201279 and 31371708), Zhejiang Provincial Natural Science Foundation (LZ14C130002), the Project of the Science and Technology Department of Zhejiang Province (No. 2013C32023, 2013C02005) and Jiangsu Collaborative Innovation Center for Modern Crop Production, P.R. China.

Author Contributions

H.J., S.M.S. and N.A. initiated, designed the research and wrote the manuscript, S.M.S., G.Y., L.J. and H.Q. performed the experiments, C.D.D., H.W.M. and N.M.Y. analyzed the data, H.J. revised and edited the manuscript and also provided advice on the experiments.

Additional Information

Supplementary information accompanies this paper at <http://www.nature.com/srep>

Competing financial interests: The authors declare no competing financial interests.

How to cite this article: Salah, S. M. *et al.* Seed priming with polyethylene glycol regulating the physiological and molecular mechanism in rice (*Oryza sativa* L.) under nano-ZnO stress. *Sci. Rep.* **5**, 14278; doi: 10.1038/srep14278 (2015).



This work is licensed under a Creative Commons Attribution 4.0 International License. The images or other third party material in this article are included in the article's Creative Commons license, unless indicated otherwise in the credit line; if the material is not included under the Creative Commons license, users will need to obtain permission from the license holder to reproduce the material. To view a copy of this license, visit <http://creativecommons.org/licenses/by/4.0/>